LBL-29082
UC-410

Center for Advanced Materials

CAM

Submitted to Surface Science

A Real-Space Multiple Scattering Theory of Low Energy Electron Diffraction: A New Approach for the Structure Determination of Stepped Surfaces

X.-G. Zhang, P.J. Rous, J.M. MacLaren, A. Gonis,
M.A. Van Hove, and G.A. Somorjai

July 1990

For Reference

Not to be taken from this room

LBL 29082 c.1

Materials and Chemical Sciences Division

Lawrence Berkeley Laboratory • University of California

ONE CYCLOTRON ROAD, BERKELEY, CA 94720 • (415) 486-4755

Prepared for the U.S. Department of Energy under Contract DE-AC03-76SF00098

DISCLAIMER

This document was prepared as an account of work sponsored by the United States Government. While this document is believed to contain correct information, neither the United States Government nor any agency thereof, nor the Regents of the University of California, nor any of their employees, makes any warranty, express or implied, or assumes any legal responsibility for the accuracy, completeness, or usefulness of any information, apparatus, product, or process disclosed, or represents that its use would not infringe privately owned rights. Reference herein to any specific commercial product, process, or service by its trade name, trademark, manufacturer, or otherwise, does not necessarily constitute or imply its endorsement, recommendation, or favoring by the United States Government or any agency thereof, or the Regents of the University of California. The views and opinions of authors expressed herein do not necessarily state or reflect those of the United States Government or any agency thereof or the Regents of the University of California.

LBL-29082

A Real-Space Multiple Scattering Theory of Low Energy Electron Diffraction: A New Approach for the Structure Determination of Stepped Surfaces

X.-G. Zhang, P.J. Rous, J.M. MacLaren[1],
A. Gonis[2], M.A. Van Hove and G.A. Somorjai

Materials and Cemical Sciences Division
Center for Advanced Materials
Lawrence Berkeley Laboratory
University of California
Berkeley, CA 949720, U.S.A.
and
University of California
Berkeley, CA 94720, U.S.A.

[1]Theoretical Division, Los Alamos National Laboratory, Los Alamos, NM 87545
[2]Division of Chemistry and Materials Science, Lawrence Livermore National Laboratory, Livermore, CA 94550

Acknowledgement: The computational work reported here was supported in part by the US Department of Energy under a *Grand Challenge* program. The project was partially supported by the Director, Office of Energy Research, Office of Basic Energy Sciences, Materials Sciences Division, US Department of Energy, under contract No. DE-AC03-76SF0098, and the Lawrence Livermore National Laboratory under contract No. W-7405-ENG-48.

ABSTRACT

A new theory of Low Energy Electron Diffraction (LEED) is presented in which the relevant multiple scattering equations are solved in the angular momentum representation within the framework of real-space multiple scattering theory (RS-MST). This approach avoids the plane wave basis used in many conventional LEED techniques and its associated limitations when applied to the calculation of LEED intensities from open surfaces containing small bulk interplanar spacings. In particular, high Miller index, stepped surfaces which lie beyond the present capabilities of conventional LEED, can now be treated in a relatively efficient and convergent manner. The new theory is tested by evaluating I-V spectra from the (100), (311), (331) surfaces of Cu which are compared with the results of a layer doubling (LD) LEED calculation. Excellent agreement is obtained in the (100) and (311) cases, for which the LD approach is expected to be applicable. The (311) surface is about the highest index fcc surface which can reasonably be attempted with the existing approaches. The results obtained for the case of the (331) surface using the LD and the RS-MST approaches agree up to about $E = 100$eV, beyond which the LD process fails to converge. We discuss and contrast the convergence properties of both methods.

I. INTRODUCTION

Steps at single-crystal surfaces are known or suspected to be important models for understanding processes in many technologies. Yet the atomic-scale structure of steps and adsorbates thereon has hardly been studied: there is a substantial lack of knowledge of interlayer spacings, bond lengths and bond angles at stepped surfaces.

Steps are a very important case of surface defects. There is ample evidence that they can strongly influence certain chemical reactions in heterogeneous catalysis, by providing active sites for bond breaking and bond formation, or even perhaps by interfering with surface diffusion[1]. Necessary reaction intermediates may well require certain step structures for their existence. Steps are also prominently implicated in crystal growth, by providing nucleation centers and by enabling an orderly growth process[1]. Steps may furthermore affect the mechanical properties of solids, through the pinning of dislocations and crack propagation.

Atomic-height steps are the prime example of defects at surfaces which can be created and controlled at will, in contrast with point defects, which exist in too many varieties. Steps are common on most experimentally-prepared surfaces. Scanning tunneling microscopy has shown [3] that they usually cover a much larger fraction of a well-prepared surface than point defects. This is because many point defects at surfaces (e.g. the emergence points of bulk screw dislocations) necessarily require surface steps for their existence: thus these point defects are accompanied at any surface by much larger step defects.

For surface studies, relatively regular arrays of steps are prepared by intentionally cutting a bulk crystalline sample at well-defined "vicinal" orientations near a close-packed crystallographic orientation. Each vicinal orientation implies a different type of step structure, e.g. terraces of variable width with (111) orientation and step faces with (100) orientation, or steps that are kinked (i.e. not straight on the atomic scale)[1,4,5].

Low-energy electron diffraction (LEED) patterns have provided considerable information on the qualitative nature of such steps[6,7]. For instance, it is found that steps on many metal surfaces often have a single-atom height, while many semiconductor surfaces tend to have a double-atom height (as is easily understood from the possible terminations of the respective bulk lattices). Field-ion microscopy (FIM)[8] and scanning tunneling microscopy (STM)[3] have delivered graphical confirmation of such results. STM has elucidated qualitative step structures at semiconductor surfaces, where ambiguities in the bulk termination lead to several a priori possible structures[9]. In addition, STM has shown how prevalent wide-terrace steps are on many surfaces that appear step-free to LEED, because of the limited instrumental response (coherence length parallel to the surface) of LEED.

The atomic-scale structure of steps and of adsorbates thereon has received little attention, compared to the structure of low-Miller index surfaces. In the case of clean stepped surfaces, only a few experiments have been able to determine atomic positions with any precision. These are primarily LEED analyses on surfaces like fcc(311) and (331), and bcc(210), (211) or (310)[2,10]: these surfaces have very narrow terraces, so that the successive steps presumably interact electronically and the terraces cannot accommodate adsorbates away from the steps.

Various kinds of theory have been applied to clean stepped surfaces, but few have attempted to optimize atomic positions. Such theories are usually empirical or semiempirical due to the geometrical complexity of steps. One study that did obtain atomic relaxations has shown that complex multilayer relaxations occur, with atomic displacements both perpendicular and parallel to the surface[11]. Such displacements have already been found experimentally in less stepped surfaces, such as fcc(311) and bcc(211)[10]. Another study analyzed possible multi-atom height structures of steps at semiconductor surfaces [12].

In the case of adsorbates on stepped surfaces, structural analyses have been performed in only a few cases. One example is the adsorption of oxygen on Cu(410), as studied by

angle-resolved photoelectron diffraction, in which the location of oxygen atoms in the step and on the terrace were determined[13]. Another example is the adsorption of CO on stepped Pd surfaces, investigated with electron-stimulated desorption - ion angular distribution (ESDIAD)[14]: the CO molecules were found to be intact and inclined from the terrace normal toward the macroscopic surface normal, but the point of adsorption (e.g. whether at the top of the step or in the in-step region) could not be determined. In certain cases (as with CO adsorption), high-resolution electron energy loss spectroscopy (HREELS) has been used to determine the mode of bonding of an adsorbate to a stepped surface[15]. A few theoretical studies of adsorption at steps have been performed, also using empirical or semiempirical methods[16].

To date, most theoretical calculations of LEED I-V spectra have been based upon a layer Korringa-Kohn-Rostoker method in which the semi-infinite surface is partitioned into layers of atoms parallel to the surface. The LEED wavefunction is described in a mixed basis; a spherical wave expansion within each atomic layer and as a set of plane waves propagating between the layers. After all intra-layer multiple scattering has been taken into account each layer can be regarded as a scatterer of plane waves, characterised by transmission and reflection matrices expressesd within a plane-wave basis. The layers can then be coupled together by solving the multiple scattering equations for the one–dimensional stack of layers to produce the reflectivity of a semi–infinite system. Techniques such as the perturbative renormalised forward scattering or the usual layer doubling can be adopted to produce exponential rates of convergence in the reflectivity. Thus, providing the scattering between layers can be described by a small number of plane waves, this approach will provide an excellent solution to the LEED problem. A detailed discussion of this solution can be found in the book by Pendry[17] and we refer the reader to this work. However, the cutoff in the plane wave basis set is often very large, leading to the inversion of large matrices and a computational bottleneck in the LEED calculation.

Unlike the angular momentum basis set, whose size is determined by the energy of the LEED electron, the plane wave basis set size is determined by the surface geometry and can vary dramatically from surface to surface on the same material.

Convergence deteriorates rapidly for surfaces with increasing Miller index, in such a way that calculations beyond the (311) surface of many fcc metals may not be feasible using conventional theory. The root cause of this effect is the fact that stepped surfaces present relatively large two-dimensional unit cells coupled with narrow interlayer spacings and low symmetry[1,5]. This combination is fatal to the otherwise efficient plane-wave expansion used in many LEED theories[17,18]. Indeed, with smaller interlayer spacings in particular, the number of plane waves that must be included grows extremely fast, while numerical convergence cannot be maintained. The most robust plane-wave algorithms, layer doubling and the Bloch-wave method[17,18], often diverge for interlayer spacings below about 1Å: for reference, Cu(331) has a bulk interlayer spacing of 0.83Å.

The difficulties associated with the closely–spaced layers can immediately be seen by examining the form of the plane wave basis functions coupling the layers. The basis functions coupling two layers separated by the vector $\mathbf{c} = (\mathbf{c}_{\parallel}, c_z)$ converge uniformly provided the z component of the interlayer spacing is non-zero, since for large 2-d reciprocal lattice vectors ($\mathbf{g}$) they take the form

$$< \mathbf{r}|\mathbf{K}_{\mathbf{g}}^{\pm} > \Big|_{\mathbf{r}=\mathbf{c}} = e^{i(\mathbf{k}+\mathbf{g})\cdot\mathbf{c}_{\parallel}+i\sqrt{2E-(\mathbf{k}+\mathbf{g})^2}|c_z|} \rightarrow e^{i(\mathbf{k}+\mathbf{g})\cdot\mathbf{c}_{\parallel}}e^{-\mathbf{g}|c_z|} \qquad \text{as } \mathbf{g} \rightarrow \infty. \quad (1)$$

where $\mathbf{k}$ is the component of the incident electron wavevector parallel to the surface. Thus, while exponentially convergent, the rate clearly depends on the size of c_z. In systems where c_z is small, many vectors are required to converge the interlayer scattering to a prescribed accuracy. Two further factors work against this basis for closely-spaced layers. First, the number of 2-d reciprocal lattice vectors scales as $|g_{\mathbf{max}}|^2$ thus exacerbating rates of convergence. Second, for surfaces with increasing Miller indices, stacking layers together

results not only in the smaller spacing between layers but also in increasing the size of the 2-d layer unit cell and hence decreasing the magnitude of the **g** vectors. Therefore, reducing the spacing c_z by half, would require the increase of $|g_{\mathbf{max}}|$ by a factor of 2, and the total number of beams needed would scale by a factor of 8, due to the larger $|g_{\mathbf{max}}|$ and the smaller reciprocal vectors, and resulting in a 216 fold increase in the computing time. These factors have limited structural determinations by LEED to low Miller index surfaces.

Conventional spherical-wave expansion methods like giant-matrix inversion [17,18] do not help much, because they lead to excessively large matrix dimensions and computing times. Typically, one would represent the surface by a finite number of atomic layers (parallel to the surface). This number grows inversely with the interlayer spacing to maintain a constant depth determined by the electronic mean-free path. And the matrix dimensions grow in proportion to the number of these layers, leading to large matrix inversion times, for instance.

Thus a new theory is needed. Several approaches have already been proposed. One is based on bundles of chains of atoms parallel to the steps[19]: first the scattering within one chain of atoms is calculated (using cylindrical waves), after which many such chains are bundled together to form a step. Two other methods combine the plane-wave and spherical-wave expansions in such a way as to generate effectively larger interlayer spacings between groups of layers[20,21], bundled together to form a step. The chain method has no requirement for periodicity within the surface and therefore has been used to evaluate diffuse LEED intensities[19]. Whilst the chain approach is ideal for dealing with disordered step arrays, its inability to exploit periodicity makes this technique relatively inefficient when applied to well ordered surfaces. Two alternative methods employ the spherical wave basis to combine together a few atomic planes and then proceed to treat the surface as a stack of these "composite" layers separated by an effectively larger interlayer spacing[20,21].

This technique improves convergence with respect to the actual interplanar spacing but still employs a plane wave basis, the number of components of which scales as the area of the surface unit cell. In effect, these methods reduce the number of evanscent waves needed in a conventional LEED calculation by increasing the effective layer spacing, at the expense of the computational effort required to build the composite layers from their constituent atomic planes.

In this work we propose a new approach to the analysis of LEED spectra that dispenses completely with plane waves (except of course in the trivial propagation through vacuum from the electron gun to the surface and back to the detector). Within the surface, it only uses spherical waves and strongly reduces the scaling problems of the earlier methods. The new approach is based on the real-space multiple scattering theory (RS-MST) which was first developed for and applied to electronic band-structure problems[22,23]. RS-MST uses the principle of the removal invariance which holds for semi-infinite periodic lattices: removing a layer from the free end of such a lattice does not change the electronic states (except for a trivial phase factor), because the resulting surface is identical to the original one being merely displaced with respect to that by a single layer. This removal invariance provides a self-consistency condition for the electronic states, which can be solved numerically. Our application to LEED will be carried out in the spirit of layer doubling, but in the spherical-wave basis rather than in the plane-wave basis. The present work will provide both more details of the method and its extension to the calculation of LEED I–V curves. In this paper, we will formulate the calculation of the surface reflectivity solely in terms of matrices evaluated in an angular momentum basis. We *stress* that the solution presented here is equally applicable to both low and high Miller index surfaces, since the use of the plane wave basis set is not needed to couple layers together. But our work is primarily aimed towards the interpretation of LEED intensities from clean or adsorbate-covered high Miller index surfaces.

II. THEORY

A. Removal Invariance

The new theory exploits the *semi–infinite periodicity* of the unrelaxed surface, and enables us to avoid the plane wave basis and its associated problems. The simplest possible surface is one of equidistant planes of atoms, and thus corresponds to the ideal bulk termination of the crystal. In general, however, the selvedge will undergo some form of restructuring, exhibiting planar relaxation perpendicular and/or parallel to the surface and perhaps reconstruction of the first few atomic layers, and may also involve adsorbates. Such deviations from the ideal semi-infinite bulk lattice can be incorporated in at least two ways. We may construct the surface of the semi-infinite ideal bulk termination joined to a slab of a few atomic planes representative of the restructured selvedge. Alternatively we can consider the actual surface as a structural distortion of the bulk termination amenable to treatment by a perturbative approach such as Tensor LEED[24,25]. Either way the crucial ingredient is a description of the ideal bulk termination. Once this has been obtained, the true surface can easily be solved as outlined above.

The bulk termination of an ideal crystal exhibits a universal property, a consequence of the semi–infinite periodicity perpendicular to the surface. In simplest terms it implies that the reflectivity of the crystal is unchanged (within a trivial phase factor) if an atomic plane is peeled away from the surface. More generally, we can say that the full scattering t-matrix of the system is invariant with respect to the removal of any finite number of layers from the surface. This *removal invariance* property is the foundation of our new approach to LEED theory. In the next section we derive an expression for the reflectivity of the entire surface within a purely angular momentum basis. We then use the removal invariance property to

construct a *self–consistent* equation for the full t–matrix, Green function and consequently the reflectivity of the surface. Finally we present a general method for the self consistent solution of this non–linear equation within an angular momentum representation.

B. The Surface Reflectivity

In this section we derive an expression for the reflectivity of a surface in a purely angular momentum basis. To this end, we consider the Schrödinger equation for the wavefunction ψ associated with an incident electron beam on a surface,

$$H\psi = E\psi \tag{2}$$

The Hamiltonian H can be split into the free-space Hamiltonian H_0 and the potential V representing the surface.

$$H = H_0 + V \tag{3}$$

The Green function associated with H_0 is

$$G_0 = (E - H_0)^{-1} \tag{4}$$

where E, which can be complex, contains an imaginary part $i\epsilon$ ($\epsilon \to 0^+$). This ensures that the correct, causal, boundary conditions are satisfied by G and related parameters entering multiple scattering theory. The corresponding wavefunction χ is the solution of

$$H_0\chi = E\chi \tag{5}$$

The (LEED) wavefunction arising from the scattering of χ by the surface potential V is given by the well-known Lippmann-Schwinger equation,

$$\psi(\mathbf{r}) = \chi(\mathbf{r}) + \int d^3\mathbf{r}' d^3\mathbf{r}'' G_0(\mathbf{r},\mathbf{r}')T(\mathbf{r}',\mathbf{r}'')\chi(\mathbf{r}'') \tag{6}$$

where T is the total (full) scattering matrix of the surface in the real space representation

$$T(\mathbf{r},\mathbf{r}'') = V(\mathbf{r})\delta(\mathbf{r}-\mathbf{r}'') + \int d^3\mathbf{r}'\ V(\mathbf{r})G_0(\mathbf{r},\mathbf{r}')T(\mathbf{r}',\mathbf{r}'') \tag{7}$$

In a LEED experiment, an incident free-electron beam of energy E and parallel momentum $\mathbf{k}_{\parallel}$ impinges upon the surface

$$\chi(\mathbf{r}) = \sum_{\mathbf{g}} U_{\mathbf{g}}^{+} e^{i\mathbf{K}_{\mathbf{g}}^{+}\cdot\mathbf{r}} \tag{8}$$

where

$$\mathbf{K}_{\mathbf{g}}^{\pm} = (\mathbf{k}_{\parallel}+\mathbf{g}, K_{\mathbf{g}z}^{\pm}) \tag{9}$$

and

$$K_{\mathbf{g}z}^{\pm} = \pm\sqrt{\kappa^2 - |\mathbf{k}_{\parallel}+\mathbf{g}|^2} \tag{10}$$

$\mathbf{g}$ is a two-dimensional reciprocal lattice vector of the surface, $\kappa = \sqrt{E}$ and the $+$ $(-)$ sign indicates the waves propagating into (out of) the surface. We use the Rydberg atomic units throughout, where 1Ry $\simeq$ 13.6 eV.

The total LEED wavefunction is then

$$\psi(\mathbf{r}) = \sum_{\mathbf{g}} U_{\mathbf{g}}^{+} e^{i\mathbf{K}_{\mathbf{g}}^{+}\cdot\mathbf{r}} + \int d^3\mathbf{r}' d^3\mathbf{r}'' G_0(\mathbf{r},\mathbf{r}')T(\mathbf{r}',\mathbf{r}'') \sum_{\mathbf{g}} U_{\mathbf{g}}^{+} e^{i\mathbf{K}_{\mathbf{g}}^{+}\cdot\mathbf{r}''} \tag{11}$$

Into this equation we now substitute the free-particle Green function expressed as an integral in a linear momentum representation

$$G_0(\mathbf{r},\mathbf{r}') = \frac{1}{(2\pi)^3}\int d^3\mathbf{k}' \frac{e^{i\mathbf{k}'\cdot(\mathbf{r}-\mathbf{r}')}}{E-|\mathbf{k}'|^2} \tag{12}$$

which upon partitioning the double integral in (11) into a summation over cell integrals can be cast in the form,

$$\psi(\mathbf{r}) = \sum_{\mathbf{g}} U_{\mathbf{g}}^{+} e^{i\mathbf{K}_{\mathbf{g}}^{+}\cdot\mathbf{r}} + \sum_{\mathbf{g}} \frac{U_{\mathbf{g}}^{+}}{(2\pi)^3} \sum_{ij} \int d^3\mathbf{r}_i' d^3\mathbf{r}_j'' d^3\mathbf{k}' \frac{e^{i\mathbf{k}'\cdot(\mathbf{r}-\mathbf{r}')}}{E-|\mathbf{k}'|^2} \tau_{ij}(\mathbf{r}_i',\mathbf{r}_j'') e^{i\mathbf{K}_{\mathbf{g}}^{+}\cdot\mathbf{r}''} \tag{13}$$

where τ_{ij} is the scattering path operator[26], defined by,

$$T = \sum_{ij} \tau_{ij} \tag{14}$$

The cell coordinates $\mathbf{r}'_i$ ($\mathbf{r}''_j$) denote the same points as $\mathbf{r}'$ ($\mathbf{r}''$) but measured with respect to an origin at the center of the corresponding cell. At this point we consider cells of arbitrary shape containing each atomic center. In practice we will make the muffin–tin approximation of spherically symmetric cells surrounded by interstitial regions of constant potential.

Since we assume that the surface is divided into layers parallel to the surface we can group the summation in (13) over layers and cells within the same layer. Thus cell i is labelled by two indices i and I, which denote cell i of layer I. In this notation then $\mathbf{R}_i$, measures the distance to the center of cell i within layer I, from the origin, $\mathbf{C}_I$, in the same layer ($\mathbf{C}_I$ would also correspond to a cell center). This leads to the expression,

$$\begin{aligned}\psi(\mathbf{r}) = &\sum_{\mathbf{g}} U^+_{\mathbf{g}} e^{i\mathbf{K}^+_{\mathbf{g}}\cdot\mathbf{r}} \\ &+ \sum_{\mathbf{g}IJ} \frac{U^+_{\mathbf{g}}}{(2\pi)^3} \int d^3\mathbf{r}'_I d^3\mathbf{r}''_J d^3\mathbf{k}' \frac{e^{i\mathbf{k}'\cdot(\mathbf{r}-\mathbf{r}'_I-\mathbf{C}_I)}}{E-|\mathbf{k}'|^2} \sum_{ij} e^{-i\mathbf{k}'\cdot\mathbf{R}_i} \tau_{I_iJ_j}(\mathbf{r}'_I,\mathbf{r}''_J) e^{i\mathbf{K}^+_{\mathbf{g}}\cdot(\mathbf{R}_j+\mathbf{r}''_j+\mathbf{C}_J)}\end{aligned} \tag{15}$$

where $\mathbf{r}_I$ is now measured with respect to the origin of cell i in layer I. The summations over i, j are within layers I, J, respectively. Note that the integrals over the unit cells are the same within each layer since 2-d periodicity has been assumed, thus allowing us to take them out of the summations over i, j.

The 2-d periodicity parallel to the surface implies that the summation over i, j in the above expression becomes

$$\frac{(2\pi)^2}{A} \sum_{\mathbf{g}'} \tau(\mathbf{k}_\parallel, \mathbf{r}'_I, \mathbf{r}''_J)\delta(\mathbf{k}'_\parallel - \mathbf{k}_\parallel - \mathbf{g}'), \tag{16}$$

where the $\mathbf{k}_{\|}$ is the component of momentum parallel to the surface, and A is the area of the surface unit cell. Integrating over $\mathbf{k}'$ we obtain an expression for the LEED wavefunction $\psi(\mathbf{r})$ in the constant potential region between any two layers N and $N+1$,

$$\begin{aligned}\psi(\mathbf{r}) = &\sum_{\mathbf{g}} U_{\mathbf{g}}^{+} e^{i\mathbf{K}_{\mathbf{g}}^{+}\cdot\mathbf{r}} \\ &- \sum_{\mathbf{g}\mathbf{g}'J} \frac{1}{2}\frac{iU_{\mathbf{g}}^{+}}{AK_{\mathbf{g}'z}} \sum_{I\leq N} e^{i\mathbf{K}_{\mathbf{g}'}^{+}\cdot(\mathbf{r}-\mathbf{C}_I)} e^{i\mathbf{K}_{\mathbf{g}}^{+}\cdot\mathbf{C}_J} \int d^3\mathbf{r}_I' d^3\mathbf{r}_J'' e^{-i\mathbf{K}_{\mathbf{g}'}^{+}\cdot\mathbf{r}_I'} \tau(\mathbf{k}_{\|}, \mathbf{r}_I', \mathbf{r}_J'') e^{i\mathbf{K}_{\mathbf{g}}^{+}\cdot\mathbf{r}_J''} \\ &- \sum_{\mathbf{g}\mathbf{g}'J} \frac{1}{2}\frac{iU_{\mathbf{g}}^{+}}{AK_{\mathbf{g}'z}} \sum_{I>N} e^{i\mathbf{K}_{\mathbf{g}'}^{-}\cdot(\mathbf{r}-\mathbf{C}_I)} e^{i\mathbf{K}_{\mathbf{g}}^{+}\cdot\mathbf{C}_J} \int d^3\mathbf{r}_I' d^3\mathbf{r}_J'' e^{-i\mathbf{K}_{\mathbf{g}'}^{-}\cdot\mathbf{r}_I'} \tau(\mathbf{k}_{\|}, \mathbf{r}_I', \mathbf{r}_J'') e^{i\mathbf{K}_{\mathbf{g}}^{+}\cdot\mathbf{r}_J''}\end{aligned} \tag{17}$$

Using the expansion of plane waves into spherical waves,

$$e^{i\mathbf{K}\cdot\mathbf{r}} = 4\pi \sum_{L} i^l j_l(\kappa r) Y_L(\hat{\mathbf{K}}) Y_{L'}^{*}(\hat{\mathbf{r}}) \tag{18}$$

where j_l is a spherical Bessel function, the integrals over the unit cells in (17) can be directly transformed into an expansion over the angular momentum states

$$\begin{aligned}\psi(\mathbf{r}) = &\sum_{\mathbf{g}} U_{\mathbf{g}}^{+} e^{i\mathbf{K}_{\mathbf{g}}^{+}\cdot\mathbf{r}} \\ &- \sum_{\mathbf{g}\mathbf{g}'J} U_{\mathbf{g}}^{+} \frac{8\pi^2 i}{AK_{\mathbf{g}'z}} \sum_{I\leq N} e^{i\mathbf{K}_{\mathbf{g}'}^{+}\cdot(\mathbf{r}-\mathbf{C}_I)} e^{i\mathbf{K}_{\mathbf{g}}^{+}\cdot\mathbf{C}_J} \sum_{LL'} i^{l'-l} Y_L(\hat{\mathbf{K}}_{\mathbf{g}'}^{+}) Y_{L'}^{*}(\hat{\mathbf{K}}_{\mathbf{g}}^{+}) \tau_{IJ}^{LL'}(\mathbf{k}_{\|}) \\ &- \sum_{\mathbf{g}\mathbf{g}'J} U_{\mathbf{g}}^{+} \frac{8\pi^2 i}{AK_{\mathbf{g}'z}} \sum_{I>N} e^{i\mathbf{K}_{\mathbf{g}'}^{-}\cdot(\mathbf{r}-\mathbf{C}_I)} e^{i\mathbf{K}_{\mathbf{g}}^{+}\cdot\mathbf{C}_J} \sum_{LL'} i^{l'-l} Y_L(\hat{\mathbf{K}}_{\mathbf{g}'}^{-}) Y_{L'}^{*}(\hat{\mathbf{K}}_{\mathbf{g}}^{+}) \tau_{IJ}^{LL'}(\mathbf{k}_{\|})\end{aligned} \tag{19}$$

where $\tau_{IJ}^{LL'}(\mathbf{k}_{\|})$ are the angular momentum matrix elements of the scattering path operator between layers I and J, given by:

$$\tau_{IJ}^{LL'}(\mathbf{k}_{\|}) = \int d^3\mathbf{r}_I' d^3\mathbf{r}_J'' j_l(\kappa r_I) Y_L(\hat{\mathbf{r}}_I) \tau(\mathbf{k}_{\|}, \mathbf{r}_I', \mathbf{r}_J'') j_{l'}(\kappa r_J) Y_{L'}^{*}(\hat{\mathbf{r}}_J) \tag{20}$$

Outside the surface the LEED wavefunction consists of the incident and reflected plane waves

$$\psi(\mathbf{r}) = \sum_{\mathbf{g}} U_{\mathbf{g}}^{+} e^{i\mathbf{K}_{\mathbf{g}}^{+}\cdot\mathbf{r}} + \sum_{\mathbf{g}'} V_{\mathbf{g}'}^{-} e^{i\mathbf{K}_{\mathbf{g}'}^{-}\cdot\mathbf{r}}, \qquad z < 0 \tag{21}$$

Now the reflection matrix of the surface R is defined as

$$V_{\mathbf{g}'}^{-} = \sum_{\mathbf{g}} R_{\mathbf{g}'\mathbf{g}}^{-+} U_{\mathbf{g}}^{+}, \tag{22}$$

and a single incident beam $\mathbf{g}$ carrying unit current the intensity reflected into each LEED beam $\mathbf{g}'$ is given by the expression,

$$I_{\mathbf{g}'} = \left| \frac{K_{\mathbf{g}'z}}{K_{\mathbf{g}z}} \right| |R_{\mathbf{g}'\mathbf{g}}^{-+}|^2 \tag{23}$$

Comparing (19) and (22) we obtain the relation between the coefficient of reflection in the *plane wave* representation, $R_{\mathbf{g}'\mathbf{g}}^{-+}$, and the scattering path operator in the *angular momentum* representation, $\tau_{IJ}^{LL'}(\mathbf{k}_{\parallel})$,

$$R_{\mathbf{g}'\mathbf{g}}^{-+} = -\frac{8\pi^2 i}{AK_{\mathbf{g}'z}^{+}} \sum_{IJ} e^{-i\mathbf{K}_{\mathbf{g}'}^{\pm}\cdot\mathbf{C}_I} e^{i\mathbf{K}_{\mathbf{g}}^{+}\cdot\mathbf{C}_J} \sum_{LL'} i^{l'-l} Y_L(\hat{\mathbf{K}}_{\mathbf{g}'}^{\pm}) Y_{L'}^{*}(\hat{\mathbf{K}}_{\mathbf{g}}^{+}) \tau_{IJ}^{LL'}(\mathbf{k}_{\parallel}). \tag{24}$$

Considering, for a moment, (24) we see that the reflectivity of the surface has been expressed in a angular momentum represenation projected onto plane wave states. In particular it is the $\tau_{IJ}(\mathbf{k}_{\parallel})$'s which contain all the information concerning the multiple scattering within the surface. This is evident from the kinematic limit in which for the case of only one atom per unit cell we have,

$$R_{\mathbf{g}'\mathbf{g}}^{-+} = -\frac{8\pi^2 i}{A\kappa K_{\mathbf{g}'z}^{\pm}} \sum_{IJ} e^{-i\mathbf{K}_{\mathbf{g}'}^{\pm}\cdot\mathbf{C}_I} e^{i\mathbf{K}_{\mathbf{g}}^{+}\cdot\mathbf{C}_J} \sum_{LL'} i^{l'-l} Y_L(\hat{\mathbf{K}}_{\mathbf{g}'}^{\pm}) Y_{L'}^{*}(\hat{\mathbf{K}}_{\mathbf{g}}^{+}) t_L^I \delta_{ll} \delta_{IJ} \tag{25}$$

where t_L^I is the *atomic t-matrix* of the atom in layer I. Comparing (24) and (25) we can clearly see that in the dynamical limit the "bare" single-center atomic t-matrices are replaced with the two-center scattering path operators $\tau_{IJ}(\mathbf{k}_{\parallel})$ which describe the complex multiple scattering paths linking the two atomic layers I and J. More importantly, we have acheived our original aim; the removal of the plane wave basis from the multiple scattering expressions and the associated calculations. Now the plane wave states are only needed

to project out the elements of $\tau_{IJ}(\mathbf{k}_{\|})$ onto the reflected and incident LEED beams, while the multiple scattering paths are summed entirely in an angular momentum basis.

Equation (24) forms the foundation of our new LEED theory. The central problem which remains is the determination of $\tau_{IJ}(\mathbf{k}_{\|})$ for the entire semi-infinite surface. It is this task which will occupy us in the next section. To simplify notation we consider only one atom-type per layer, so that the site labels refer to atoms rather than unit cells. The generalisation to many atoms per cell is straightforward. In this case extra indices labelling inequivalent atoms within each cell are needed.

C. The Self-Consistent Equation

The scattering path operator, τ_{ij}, connecting cells i and j among a collection of scatterers can be related to the atomic scattering t-matrices, t_i, by the so-called the equation of motion[26],

$$\tau_{ij} = t_i \delta_{ij} + \sum_{k \neq j} t_i G_{ik} \tau_{kj}, \tag{26}$$

where G_{ik} are the propagators (structure constants) between cells i and k. We regard each quantity in (26) as a matrix with indices LL' associated with angular momentum states. We now make use of the two-dimensional periodicity parallel to the surface and use a lattice Fourier transformation to obtain,

$$\tau_{IJ}(\mathbf{k}_{\|}) = [\eta_{\mathrm{ay}}(\mathbf{k}_{\|})]_I \delta_{IJ} + [\eta_{\mathrm{ay}}(\mathbf{k}_{\|})]_I \sum_{K \neq J} G_{IK}(\mathbf{k}_{\|}) \tau_{KJ}(\mathbf{k}_{\|}), \tag{27}$$

where upper case subscripts are layer indices and an isolated layer is represented by the quantity,

$$[\eta_{\mathrm{ay}}(\mathbf{k}_{\|})]_I^{-1} = t_I^{-1} - G_{II}(\mathbf{k}_{\|}), \tag{28}$$

with the interplanar (and intraplanar when $I = J$) propagators defined as

$$G_{IJ}(\mathbf{k}_{\|}) = \frac{1}{N}\sum_{i,j} G(\mathbf{R}_{ij})e^{i\mathbf{k}\cdot\mathbf{R}_{ij}}, \quad i \text{ in layer } I \text{ and } j \text{ in layer } J, \tag{29}$$

where N is the number of unit cells in the layer and the limit $N \to \infty$ is taken. Therefore, the formal solution for $\tau_{IJ}(\mathbf{k}_{\|})$ from (28) is the inverse of the matrix,

$$[\tau(\mathbf{k})^{-1}]_{IJ} = [\tau_{\text{lay}}(\mathbf{k})]_I^{-1}\delta_{IJ} - G_{IJ}(\mathbf{k}), \tag{30}$$

For layered systems, the inversion of (27) is an effective one-dimensional problem for each incident beam direction. In a conventional plane wave basis this inversion can be accomplished approximately by the layer doubling technique.

In the angular momentum representation the appropriate approach is to obtain a self-consistency condition to determine the reflectivity of the half solid. To do this we use the property of removal invariance in the presence of semi-infinite periodicity[22]. We imagine replacing the half solid with a single *renormalised* layer which is constructed in such a way as to possess the scattering properties of the entire half solid. In practice, a more rapidly convergent procedure is to consider a stack of layers, $I = 1, \ldots, N$, with the Nth (deepest) layer being renormalized and the remaining $N-1$ layers being bare atomic planes described by τ_{lay}. Typically we need only 2 or 3 layers to represent the entire half solid as will be made clear later in this paper.

This stack of layers is described by a matrix, $\mathcal{T}$, with both angular momentum and layer indices. Adding one more bare layer, τ_{lay}, to the top of the stack, we obtain a system represented by the $N+1$ layers,

$$\mathcal{T}_{+1} \equiv \begin{pmatrix} \tau_{\text{lay}}^{-1} & -\hat{\mathrm{G}} \\ -\hat{\mathrm{G}}' & \mathcal{T}^{-1} \end{pmatrix}^{-1} \tag{31}$$

where $\hat{\mathrm{G}}$ ($\hat{\mathrm{G}}'$) is the row (column) vectors formed from the interlayer propogators between the layer represented by $\tau_{\mathrm{lay}}(\mathbf{k}_{\|})$ and those represented by $\mathcal{T}(\mathbf{k})$, and are given by

$$\hat{\mathrm{G}} \equiv (G_{01}(\mathbf{k}_{\|}), G_{02}(\mathbf{k}_{\|}), \ldots, G_{0N}(\mathbf{k}_{\|})), \tag{32}$$

and a similar construct for the column vector $\hat{\mathrm{G}}'$. The property of removal invariance implies that this $N+1$ layer stack should represent the same half solid as the original N layer stack. Symbolically,

$$\mathcal{T}_{+1} \equiv \mathcal{T} \tag{33}$$

A schematic representation of this equation is shown in Fig. 1. Equation (33) forms the basis of our self-consistency condition for $\mathcal{T}$. However, we note that in a mixed site-angular momentum representation the dimension of $\mathcal{T}_{+1}$ is larger than that of $\mathcal{T}$ since $\mathcal{T}_{+1}$ represents a stack of $N+1$ layers and $\mathcal{T}$ a stack of only N layers. A proper equation can be obtained if we fold the two layers furthest from the surface (the renormalized layer and the layer immediately above it) into a new layer to obtain a N layer stack which is identical to the original stack. Therefore, we have a self-consistent equation for the matrix $\mathcal{T}$,

$$\mathcal{T}(\mathbf{k}) = \begin{pmatrix} I & 0 & \cdots & 0 & 0 \\ 0 & I & \cdots & 0 & 0 \\ \vdots & \vdots & \ddots & \vdots & \vdots \\ 0 & 0 & \cdots & I & g(-\mathbf{R}_{01}) \end{pmatrix} \begin{pmatrix} \tau_{\mathrm{lay}}(\mathbf{k})^{-1} & -\hat{\mathrm{G}} \\ -\hat{\mathrm{G}}' & \mathcal{T}(k)^{-1} \end{pmatrix}^{-1} \begin{pmatrix} I & 0 & \cdots & 0 \\ 0 & I & \cdots & 0 \\ \vdots & \vdots & \ddots & \vdots \\ 0 & 0 & \cdots & I \\ 0 & 0 & \cdots & g(-\mathbf{R}_{10}) \end{pmatrix} \tag{34}$$

where $g(-\mathbf{R}_{IJ})$ is the angular momentum representation of the translation operator associated with the vector $\mathbf{R}_{IJ}$ which connects the origins of the layers I and J. This quantity satisfies the property,

$$g(-\mathbf{r})G(\mathbf{R}) = G(\mathbf{R})g(-\mathbf{r}) = G(\mathbf{R}+\mathbf{r}), \quad |\mathbf{R}| > |\mathbf{r}| \tag{35}$$

The rectangular matrices,

$$\mathcal{G} = \begin{pmatrix} I & 0 & \cdots & 0 & 0 \\ 0 & I & \cdots & 0 & 0 \\ \vdots & \vdots & \ddots & \vdots & \vdots \\ 0 & 0 & \cdots & I & g(-\mathbf{R}_{01}) \end{pmatrix}, \tag{36}$$

in Eq. (34) and the corresponding matrix $\mathcal{G}'$ are called contraction matrices[27], because they reduce a given square matrix with dimension given by the number of columns of $\mathcal{G}$ to one with the dimension of the number of rows of $\mathcal{G}$. Utilizing the contraction matrices and the property of removal invariance, we transform the problem of finding the reflectivity of an infinite number of layers into one for a finite number of layers. It now only remains to solve (34) for $\mathcal{T}(\mathbf{k})$.

D. Solution of the Self-Consistent Equation

The problem of solving the non-linear matrix equation, Eq. (34), can be formulated as finding the zeroes of the matrix function

$$\mathcal{F}(\mathcal{T}) = \mathcal{T} - \mathcal{G} \begin{pmatrix} \mathcal{M} & -\hat{\mathrm{G}} \\ -\hat{\mathrm{G}}' & \mathcal{T}^{-1} \end{pmatrix}^{-1} \mathcal{G}' \tag{37}$$

with an initial guess $\mathcal{T}^{(0)}$. We now present a fast iteration scheme[27] for the solution of Eq. (37) based on the Newton-Raphson method. The derivative of the equation can be written formally as the sum of two direct products,

$$\begin{aligned} \mathcal{F}' &= \mathcal{I} \otimes \mathcal{I} \\ &- \mathcal{G} \begin{pmatrix} \mathcal{M} & -\hat{\mathrm{G}} \\ -\hat{\mathrm{G}}' & (\mathcal{T}^{(n)})^{-1} \end{pmatrix}^{-1} \begin{pmatrix} 0 \\ (\mathcal{T}^{(n)})^{-1} \end{pmatrix} \otimes \begin{pmatrix} 0 & (\mathcal{T}^{(n)})^{-1} \end{pmatrix} \begin{pmatrix} \mathcal{M} & -\hat{\mathrm{G}} \\ -\hat{\mathrm{G}}' & (\mathcal{T}^{(n)})^{-1} \end{pmatrix}^{-1} \mathcal{G}' \end{aligned} \tag{38}$$

We recall that the Newton-Raphson method for solving a matrix equation, $\mathcal{F}(x) = 0$, where $\mathcal{F}$ is a matrix function of the matrix unknown x, consists in the iteration of the equation

$$x^{(n+1)} = x^{(n)} - \mathcal{F}'(x^{(n)})^{-1} \cdot \mathcal{F}(x^{(n)}), \tag{39}$$

where $\mathcal{F}'(x)$ is the derivative of $\mathcal{F}(x)$ with respect to x. The roots of $\mathcal{F}(x)$ are given by the converged values, $x^{(\infty)}$. If we define $D^{(n)} = x^{(n)} - x^{(n+1)}$, then $D^{(n)}$ can be solved from the equation $\mathcal{F}(x^{(n)}) = \mathcal{F}'(x^{(n)}) \cdot D^{(n)}$. Therefore the solution of (39) can be obtained by iterating

$$\mathcal{T}^{(n+1)} = \mathcal{T}^{(n)} - \mathcal{D}^{(n)} \tag{40}$$

where the correction term $\mathcal{D}^{(n)}$ can be determined from the solution of the equation,

$$\begin{aligned}\mathcal{F}(\mathcal{T}^{(n)}) &= \mathcal{D}^{(n)} \\ &-\mathcal{G}\begin{pmatrix} \mathcal{M} & -\hat{\mathrm{G}} \\ -\hat{\mathrm{G}}' & (\mathcal{T}^{(n)})^{-1} \end{pmatrix}^{-1} \begin{pmatrix} 0 \\ (\mathcal{T}^{(n)})^{-1} \end{pmatrix} \mathcal{D}^{(n)} \begin{pmatrix} 0 & (\mathcal{T}^{(n)})^{-1} \end{pmatrix} \begin{pmatrix} \mathcal{M} & -\hat{\mathrm{G}} \\ -\hat{\mathrm{G}}' & (\mathcal{T}^{(n)})^{-1} \end{pmatrix}^{-1} \mathcal{G}'\end{aligned} \tag{41}$$

We now see that the original problem has been converted to one requiring the solution of a linear equation of the form

$$x - AxB = F \tag{42}$$

where x is the unknown matrix (i.e., $D^{(n)}$ in (41), and A, B and F are constant matrices which can be readily evaluated from (41). Although this equation can be solved by the time consuming inversion of the matrix $I \otimes I - A \otimes B$, a much more efficient approach is to diagonalize matrices A and B,

$$A = P\alpha P^{-1}, \quad B = Q\beta Q^{-1} \tag{43}$$

where α and β are diagonal matrices with elements $\alpha_i\delta_{ij}$ and $\beta_i\delta_{ij}$, respectively; then a change of variable $x' = P^{-1}xQ$ leads to the equation,

$$x' - \alpha x'\beta = F' \tag{44}$$

where $F' = P^{-1}FQ$. Now, the solution of the original equation becomes straightforward,

$$\begin{aligned} x'_{ij} &= \frac{F'_{ij}}{1 - \alpha_i\beta_j} \\ x &= Px'Q^{-1} \end{aligned} \tag{45}$$

E. Convergence

In this section we wish to discuss the convergence of our new theory with respect to the angular momentum expansions in the self–consistent equation, Eq. (34). Consider first the question of the scattering of electrons from a single object such as an atom. The potential, in this case, is spatially bounded and at LEED energies one can argue that those partial waves are scattered most prominently whose angular momentum, l, is less than the classical angular momentum $\sim \sqrt{E}R$, where R corresponds to the radial extent of the scatterer. Thus, only spherical waves for which $l < \sqrt{E}R$ enter the description of the scattering process. The matrix elements of the atomic t–matrix associated with higher angular momentum states fall off rapidly to zero thus allowing l truncations at $l_{\mathrm{max}} \sim \sqrt{E}R$. In the calculation of the slab T matrix, found by inverting equation (30), all l values can be truncated at the atomic l_{max}. This can most easily be justified by generating the multiple scattering series, found by iterating the scattering path operator equation of motion, Eq. (26), and observing that each term involves products of Green's functions with atomic t–matrices sandwiched in between. Indeed, the slab could in principle be made as large as possible, providing that the corresponding matrix could be inverted, with the same l truncation at the atomic value. However, in the solution of the self–consistent equation, Eq. (34), a similar multiple scattering expansion involves the products gG, given by Eq. (35), which replaces the exact Green's function for the layers separated beyond the maximum spacing inside the cluster. This product contains an internal l summation, which does not have an atomic t factor to justify a truncation. We note that this problem does not arise in the plane wave expansion for interlayer propagation since the Green's functions are diagonal in the plane wave basis. However, provided that the argument of g is smaller than that of G, formally the products are uniformly convergent in the angular momentum expansion.

Upon expanding Eq. (34), to generate a multiple scattering series, we find that the solution treats exactly all multiple scattering paths within any N nearest neighbor layers, with all multiple scattering terms between layers further apart represented by the products of Green's functions, which involve internal summations over angular momentum states that are truncated at a finite l. We can further improve this treatment by ensuring that the equation exactly reproduces all terms up to and including scatterings within $N+1$ layers by defining

$$g(-\mathbf{R}_{01}) = [G_{0n}(\mathbf{k})]^{-1} G_{0,n+1}(\mathbf{k}) \tag{46}$$

with an analogous construction for $g(-\mathbf{R}_{10})$. This implies that g is now $\mathbf{k}$ dependent. The Green's functions, at complex energy, have an exponential tail arising from the spherical Hankel functions, and thus it is more important to have an accurate calculation of nearer, rather than more distant interplanar Green's functions, which is what equation (46) achieves. Furthermore, we have found that this condition is numerically superior to performing a $N+1$-layer calculation with the exact matrix elements of g, although both reproduce the exact multiple scattering terms within any $N+1$ nearest neighbor layers. One possible reason for this is that the renormalisation of g, specified by equation (46), may improve the unitarity condition $g(-\mathbf{R}_{01})g(-\mathbf{R}_{10}) = I$, by including, in a self–consistent manner, the contributions of the neglected higher angular momentum channels. The complexity of the equations, though, makes it hard to provide any rigorous justification of this empirical observation. In essence, convergence is ensured provided that the bare cluster of N sites is a sufficiently good approximation to the true semi–infinite system. Then, the iterative solution to the non–linear self–consistent equation (34) is well behaved. Extensive numerical tests at both LEED and band energies indicate that with the constraint on g represented by equation (46), acceptable convergence is attained for $N \geq 2$ with l truncated at the atomic value. There is a balance, however, between the

cluster size and the l truncation with smaller clusters typically needing larger l basis sets and vice–versa. In the case of more open surfaces, characterized by closely-spaced layers, we have found that a few more layers may be required. This is not too surprising. For high Miller index surfaces, atoms in two layers a few interplanar spacings apart can still be close to each other thus contributing strongly to the multiple scattering effects. Therefore, errors made in approximating the Green's functions connecting these sites will tend to be more important. One can estimate the number of layers needed from the following simple relation:

$$N c_z \sqrt{\mathrm{Im}\ E} \sim \text{constant} \tag{47}$$

In this equation N, c_z, E refer to the "bare" cluster size, z–component of the interplanar spacing and the LEED electron energy (which is complex). As mentioned above, N=2 with l truncated at the atomic value is sufficient for most close packed surfaces. This establishes a scaling relation between the number of layers, N, to be used in representing the half solid and the interplanar spacing. However, the resulting increase in N for high Miller index surfaces is slow and nowhere near as dramatic as the increase in plane wave basis set size encountered in the conventional LEED theory. For example, halving the interplanar spacing would require the inclusion of at most twice the number of layers in the self–consistent equation. Therefore the dimension of the whole matrix is scaled by a factor of 2 and the computation time is scaled by a factor of $2^3 = 8$, a rather affordable factor compared with the factor of 216 for the plane wave expansion, as discussed in the introduction.

III. RESULTS

In this section we present LEED I–V spectra for Cu fcc surfaces obtained with the new RS-MST as well as conventional LEED theory. In all calculations the atomic Cu phase shifts are obtained from solving the Schrödinger equation for the potential provided by Moruzzi, Janak and Williams[28]. We found that six atomic phase shifts ($l_{\max} = 5$) were sufficient for energies below 70eV, and $l_{\max} = 6$ was required from 70eV to 200eV. In the RS-MST calculations, the angular momentum expansions for the "bare" layers (i.e., the elements of the t–matrix corresponding to the first $N-1$ layers in the self–consistency condition) were truncated at the atomic $l_{\max}$, while the truncation for the renormalized layer, layer N, is $l_{\max}+1$ to improve convergence. We used $N = 2$ for the (100) surface, $N = 3$ for the (311) surface, and $N = 4$ for the (331) surface in Eq. (34), roughly corresponding to the scaling law Nc_z =constant (Eq. (47)) where c_z is the z-component of the interplanar spacing. To further improve the speed and accuracy in the RS-MST calculations, we used explicitly the mirror symmetry which exists in all surfaces studied. In the layer doubling calculations, no symmetry was utilized.

Figure 2 shows I–V curves for (00) and (10) LEED beams calculated for a Cu(100) surface using both the layer doubling and the real-space multiple scattering theory methods. The results obtained are in excellent agreement over the whole energy range, illustrating the accuracy of the new approach. Similar I–V curves have been calculated for Cu(311) and are illustrated in Fig. 3. This system has an interplanar spacing of about 1.09Å. The comparison between the LEED results and those obtained from the RS-MST calculation are in good agreement, although some numerical difficulties were encountered at the high energy end of the spectrum, at $E \approx 165$eV. These seem to be associated with errors in the calculation of the interplanar propagators, Eq. (29), which is currently evaluated through

a real space summation, and becomes less accurate at high energies. This affects the stability of (34). This instability may be amplified by the matrix inversion subroutines used to evaluate the translation operator, Eq. (46). These difficulties may be avoided by using a more stable inversion algorithm such as singular value decomposition rather than the more usual LU decompositiom, and better schemes of calculating the interplanar propagators.

In Fig. 4, we present I-V curves for the Cu(331) surface, with an interplanar spacing of 0.83Å, obtained through both the layer doubling and the new approach. In this case the layer doubling results show some indication of numerical instability near Bragg peaks, $E \approx 50$eV, and the convergence of the layer doubling process becomes very sluggish, eventually failing to converge at some energies, e.g., $E \approx 120$eV. For other energies near this region the intensity shows rather oscillatory behavior and occasional spikes, whose width is less than the minimum allowed, which is dictated by the imaginary part of the energy. The layer doubling and RS-MST results agree well up to this point, where the disagreement becomes evident (dashed vs. solid line). However, again due to inaccuracies in obtaining the interplanar propagators, as in the case of (311) surface, at high energies, $E > 130$eV, numerical instabilities prevented us from obtaining accurate solutions of (34).

We estimated the computing time on a CRAY-2 computer by various schemes. At the low energy end of the spectrum, $E \approx 35$eV, for a Cu(311) surface, the number of beams (plane waves) needed in a layer doubling calculation is about 71, and the computing time is about 18 seconds per energy. The same calculation for the Cu(331) surface requires 153 beams and takes about 85 seconds per energy. The symmetrized RS-MST calculations at 35eV with a 3-layer ($N = 3$) self-consistency condition for the (311) surface takes about 35 seconds per energy. For the (331) surface it is necessary to use a 4-layer calculation, which takes about 65 seconds per energy. At the high end of the spectrum, $E > 150$eV, the layer doubling calculations for the (311) surface require 99 beams and 35 seconds per energy, respectively. According to the scaling law discussed after Eq. (1), the layer

doubling calculation for a (331) surface requires 199 beams and about 4 minutes per energy. However, because of an insufficiently small decay factor, the process does not converge. In the case of the RS-MST approach, the computing time for a 3-layer, $l_{\max} = 6$ calculation for the (311) surface at $E \approx 150$eV is about 75 seconds per energy. A 4-layer calculation necessary for the (331) surface roughly doubles that time.

IV. DISCUSSION

In this paper we have presented a new method for the calculation of LEED I–V curves. The technique is based on equations expressed entirely in terms of matrices in the angular momentum representation. A self–consistent equation for characterising the scattering of electrons from a semi–infinite periodic half–space (surface) has been derived and stable algorithms for obtaining solutions of this non–linear equation have been presented. The technique, unlike conventional LEED theory, is equally applicable to both low and high Miller index surfaces since increase of the matrix size associated with decreasing inter-planar spacing are much more modest than in conventional LEED calculations. The new method has been tested on Cu (100), (311) and (331) stepped surfaces where excellent agreement between old and new methods was obtained. The (311) surface is probably the highest Miller index surface which can be analysed reasonably within the conventional LEED theory, taking into account the possibility of layer relaxations and stronger multiple scattering in some metals. In the case of the (331) surface, the computation time for the RS-MST method is comparable to that of the layer doubling method, but in this case the latter begins to show difficulties of convergence.

Numerical difficulties were encountered at high energies ($E \approx 165$eV) in the RS-MST calculations for high Miller index surfaces. We believe that these difficulties were caused

by instabilities of the numerical schemes used in the calculations, and they are not inherent in the method itself. Schemes for improving the numerical aspects of the calculation are currently under consideration. At the same time, because there are more beams for each energy in the case of high Miller index surfaces, a lower energy range may be sufficient for a complete determination of the stucture of the surface. In addition, one may also use "rocking curves" (intensity versus incident beam angles) instead of IV spectra and so one may have to perform calculations at only one energy point.

The computation time of RS-MST scales more favorably than that of layer doubling, as discussed at the end of Section II and demonstrated by the numerical calculations. Yet the computation time still increases considerably as the Miller index increases. However, the substrate calculation, which is the topic of this paper, is done only once before any surface geometrical modifications like relaxation or adsorbates are added. The substrate reflection can be used again and again as the surface structure is varied through many geometries.

We note again that there is no underlying conceptual barrier for the application of the RS-MST method to high index stepped surfaces, in contrast to the limitations associated with the use of a plane wave basis. Therefore, this method provides an extremely promising way for providing accurate structural determination of stepped surfaces.

ACKNOWLEDGEMENT

The computational work reported here was supported in part by the US Department of Energy under a *Grand Challenge* program. The project was partially supported by the Director, Office of Energy Research, Office of Basic Energy Sciences, Materials Sciences Division, US Department of Energy, under contract No. DE-AC03-76SF0098, and the Lawrence Livermore National Laboratory under Contract No. W-7405-ENG-48.

V. REFERENCES

1. G.A. Somorjai, **Chemistry in Two Dimensions: Surfaces** (Cornell University Press, Ithaca, 1981).
2. J.M. MacLaren, J.B. Pendry, P.J. Rous, D.K. Saldin, G.A. Somorjai, M.A. Van Hove and D.D. Vvedensky, **Surface Crytallographic Information Service – A Handbook of Surface Structures**, (Reidel, Dordrecht, 1987)
3. D.F. Ogletree, C. Ocal, B. Marchon, G.A. Somorjai and M. Salmeron, J. Vac, Sci. Technol., in press.
4. B. Lang, R.W. Joyner and G.A. Somorjai, Surf. Sci. 30, 454 (1972).
5. M.A. Van Hove and G.A. Somorjai, Surf. Sci. 92, 489 (1980).
6. G.-C. Wang and M.G. Lagally, Surf. Sci. 81, 69 (1979).
7. M. Henzler, Surf. Sci. 22, 12 (1970).
8. E.W. Müller, Z. Phys. 136, 131 (1951); E.W. Müller and T.T. Tsong, **Field Ion Microscopy** (American Elsevier, New York) 1969; G. Ehrlich, Surf. Sci. 63, 422 (1977).
9. P.E. Wierenga, J.A. Kubby and J.E. Griffith, Phys. Rev. Letters 59, 2169 (1987).
10. A recent tabular summary of LEED and other results is available: F. Jona and P.M. Marcus, in **The Structure of Surfaces II**, eds. J.F. van der Veen and M.A. Van Hove, Springer-Verlag (Heidelberg, 1988), p. 90.
11. G. Allan, Surf. Sci. 85, 37 (1979); P.M. Marcus, P. Jiang and F. Jona, in **The Structure of Surfaces II**, eds. J.F. van der Veen and M.A. Van Hove, Springer-Verlag (Heidelberg, 1988), p. 100.
12. D.J. Chadi, Phys. Rev. Letters 59, 1691 (1987).
13. K.A. Thompson and C.S. Fadley, Surf. Sci. 146, 281 (1984).

14. T.E. Madey, J.T. Yates, Jr., A.M. Bradshaw and F.M. Hoffmann, Surf. Sci. 89, 370 (1979).

15. S. Lehwald and H. Ibach, Surf. Sci. 89, 425 (1979).

16. H. Kobayashi, S. Yoshida, H. Kato, K. Fukui and K. Tarama, Surf. Sci. 79, 189 (1979); H. Kobayashi, S. Yoshida and M. Yamaguchi, Surf. Sci. 107, 321 (1981); J.P. Jardin, M.C. Desjonquères and D. Spanjaard, J. Phys. C18, 5759 (1985).

17. J.B. Pendry, **Low Energy Electron Diffraction**, (Academic Press, London, 1974).

18. M.A. Van Hove, W.H. Weinberg and C.-M. Chan, **Low-Energy Electron Diffraction: Experiment, Theory and Surface Structure Determination** (Springer-Verlag, Heidelberg, 1986).

19. P.J. Rous and J.B. Pendry, Surf. Sci. 173, 1 (1986).

20. D.W. Jepsen, Phys. Rev. B22, 5701 (1980).

21. P. Pinkava and S. Crampin, submitted to Surf. Sci.

22. X.-G. Zhang and A. Gonis, Phys. Rev. Letters 62, 1161 (1989).

23. J.M. MacLaren, X.-G. Zhang and A. Gonis, Phys. Rev. B40, 9955 (1989).

24. P.J. Rous, J.B. Pendry, D.K. Saldin, K. Heinz, K. Müller and N. Bickel, Phys. Rev. Lett. 57, 2951 (1986).

25. P.J. Rous and J.B. Pendry, Surf. Sci. 219, 355 (1989); ibid 219, 373 (1989).

26. B.L. Gyorffy and M.K. Stott, in **Band Structure Spectroscopy of Metals and Alloys**, edited by D. J. Fabian and L. M. Watson (Academic, New York, 1973), p. 385.

27. X.-G. Zhang, Ph.D. thesis, Northwestern University (1989).

28. V.L. Moruzzi, J.F. Janak and A.R. Williams, **Calculated Electronic Properties of Metals** (Pergamon, New York, 1978).

FIGURE CAPTIONS

Fig. 1. Schematic illustration of Eq. (33). Here $N = 3$, and the quantities $\mathcal{T}$ and $\mathcal{T}_{+1}$ represent stacks of 3 and 4 layers, respectively.

Fig. 2. Comparison of LEED intensities of the Cu(100) clean surface obtained by the layer doubling (LD) and the RS-MST method, (a) (00) beam and (b) (10) beam. The solid curves depict the results of RS-MST and the dashed curves depict the results of layer doubling.

Fig. 3. Comparison of LEED intensities of the Cu(311) clean surface obtained by the layer doubling (LD) and the RS-MST method, (a) (00) beam, (b) (10) beam and (c) $(\bar{1}0)$ beam. The solid curves depict the results of RS-MST and the dashed curves depict the results of layer doubling.

Fig. 4. Comparison of LEED intensities of the Cu(331) clean surface obtained by the layer doubling (LD) and the RS-MST method, (a) (00) beam, (b) (10) beam and (c) $(\bar{1}0)$ beam. The solid curves depict the results of RS-MST and the dashed curves depict the results of layer doubling.

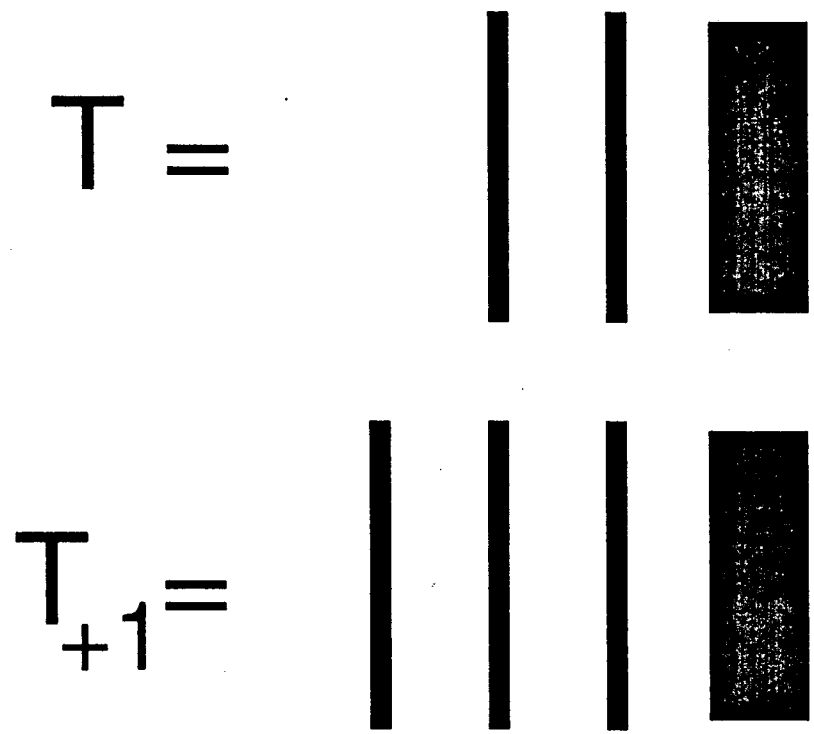

Fig. 1

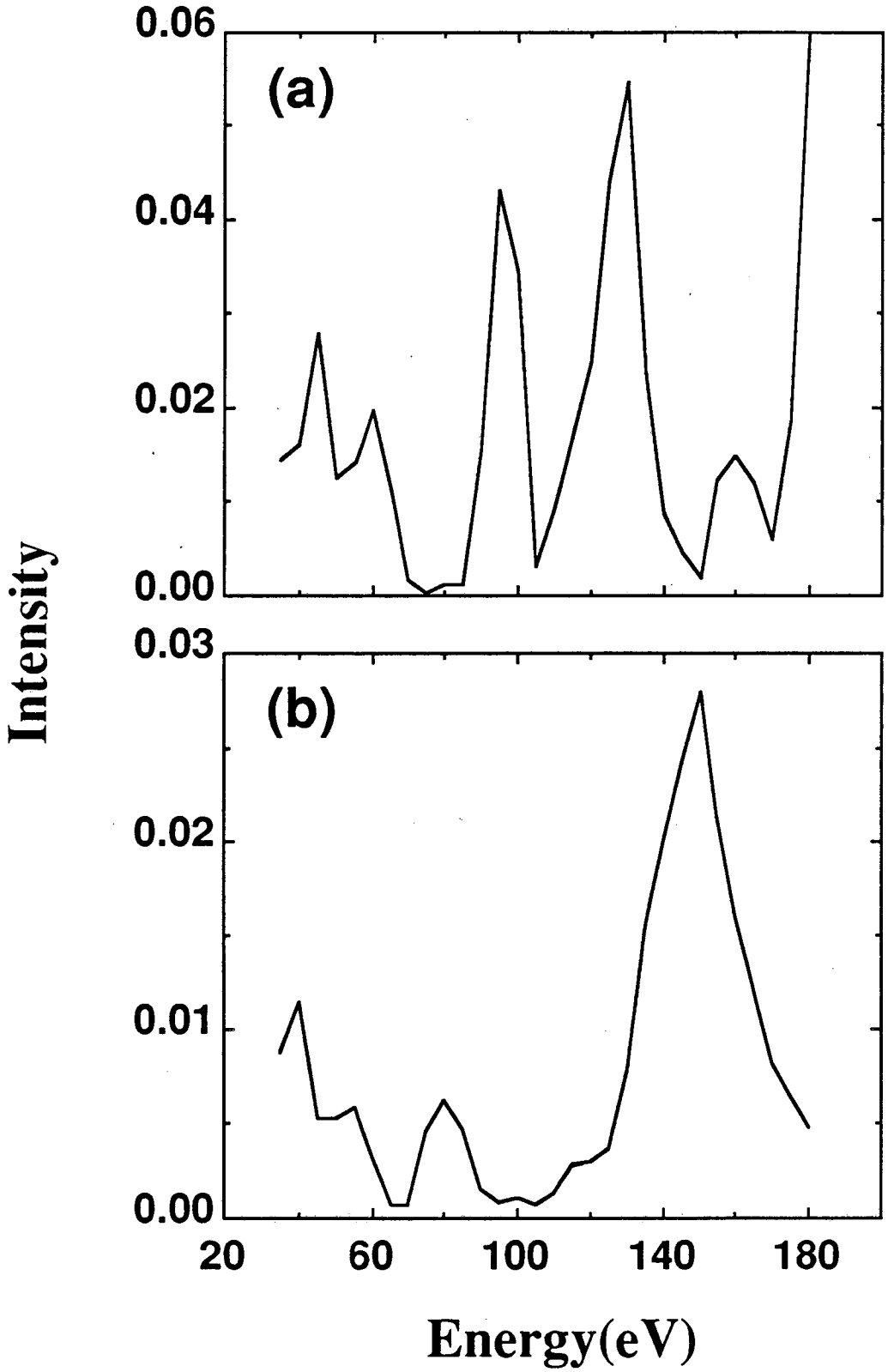

XBL 902-653

Fig. 2

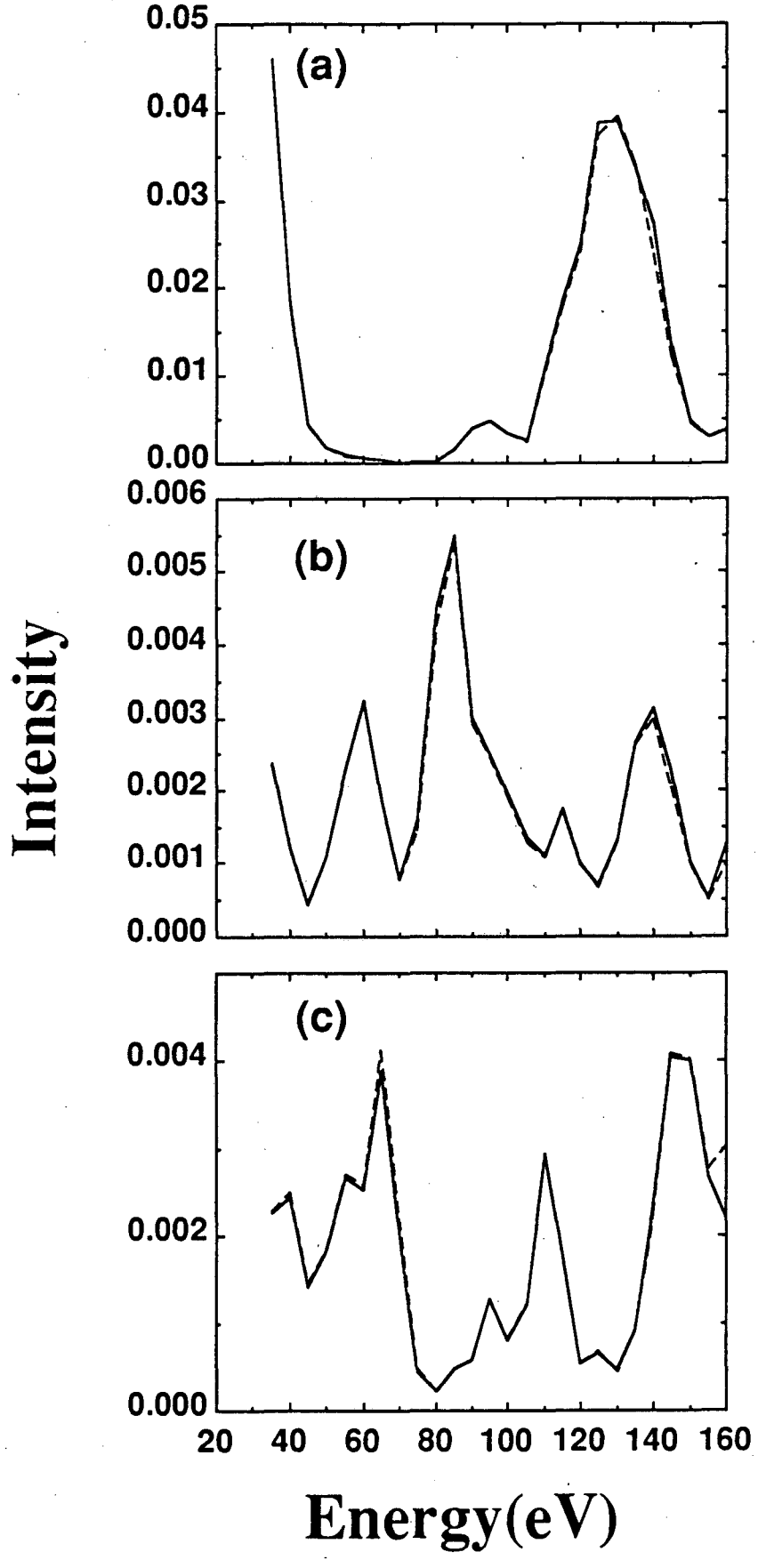

XBL 902-654

Fig. 3

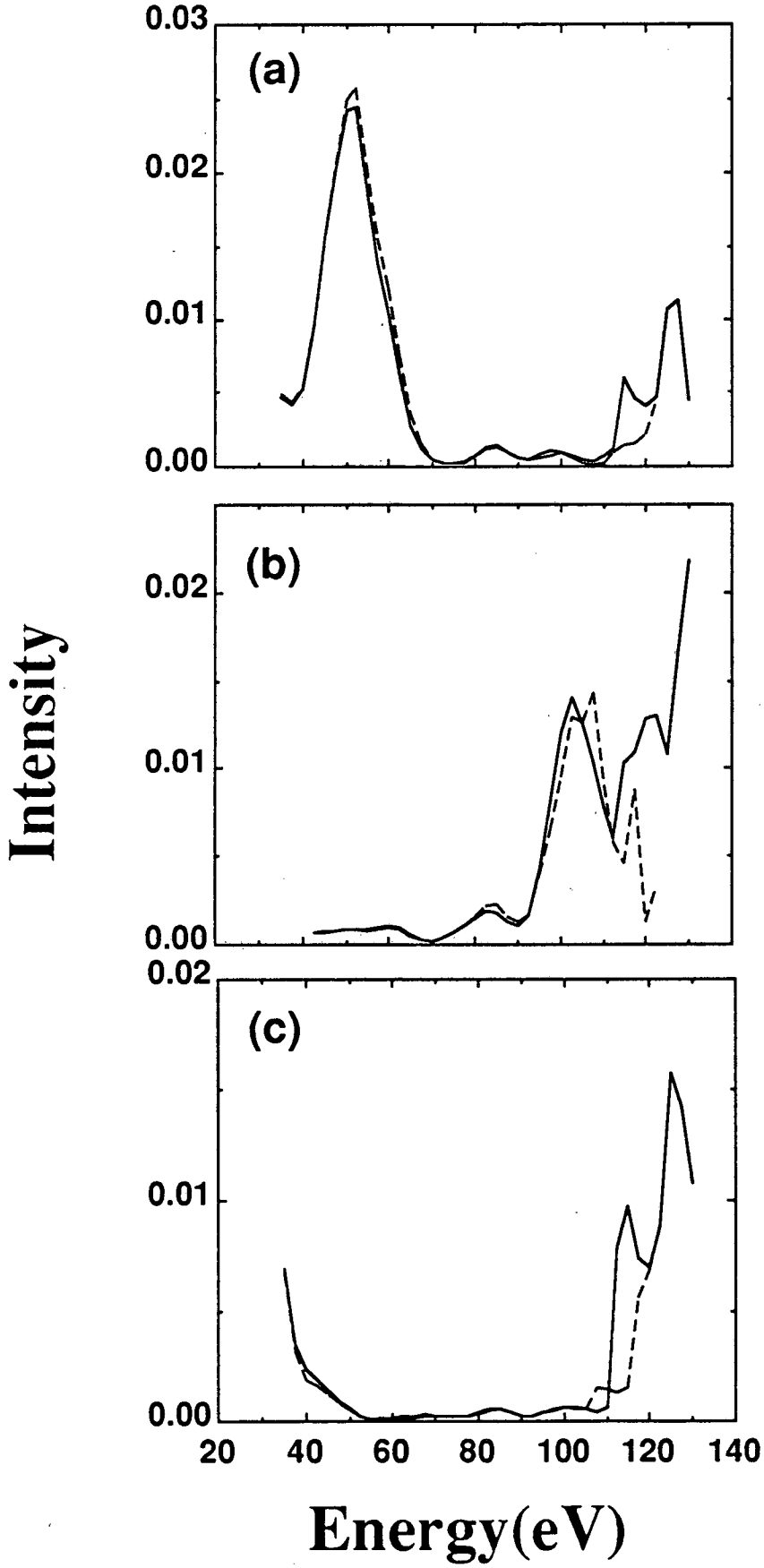

XBL 902-655

Fig. 4

LAWRENCE BERKELEY LABORATORY
CENTER FOR ADVANCED MATERIALS
1 CYCLOTRON ROAD
BERKELEY, CALIFORNIA 94720